J. Min. Metall. Sect. B-Metall. 57 (1) (2021) 83 - 96

Journal of Mining and Metallurgy, Section B: Metallurgy

PREPARATION OF NiCr/YSZ TWO-LAYERED BURN-RESISTANT COATING ON γ-TiAl ALLOYS BASED ON PLASMA SURFACE METALLURGY AND ION PLATING METHODS

D.-B. Wei [a,b,*], M.-F. Li [a,b,#], X. Zhou [a,b], F.-K. Li [a,b], S.-Q. Li [a,b], P.-Z. Zhang [a,b]

[a] College of Materials Science and Technology,
Nanjing University of Aeronautics and Astronautics, Nanjing, China
[b] Materials Preparation and Protection for Harsh Environment Key Laboratory of
Ministry of Industry and Information Technology, Nanjing, China

(Received 02 September 2020; Accepted 22 December 2020)

Abstract

The NiCr/YSZ coating was fabricated on γ-TiAl alloy by double glow plasma surface metallurgy technology and multi-arc ion plating technology. The microstructure,microhardness, bonding strength, and burn resistance of NiCr/YSZ coating were studied in detail. The results showed that the NiCr/YSZ coating was dense and homogeneous, including a duplex structure of top YSZ ceramic coating and underlying Ni-Cr bond coating. The average microhardness of NiCr/YSZ coating was raised by a factor of about 2 compared to the γ-TiAl substrate. The thermal shock test indicated that the composite structure had superior bonding strength and the defects such as metal droplets on the ceramic coating were the source of cracks. The high-energy laser beam destroyed the surface of γ-TiAl alloy, forming protruding combustion products in ablation zone and splashing residues around ablation zone. When coated by NiCr/YSZ coating, the combustion process was delayed through isolating and dissipating heat. The ablation range was controlled and the ablation damage was reduced at the same irradiation power. The NiCr/YSZ coating preliminarily realized to improve the burn resistance of γ-TiAl alloy.

Keywords: *γ-TiAl alloys; NiCr/YSZ coating; Microstructure; Bonding strength; Burn resistance*

1. Introduction

With recent developments in different technologies, the investigation of materials confronting in extreme working conditions has become a research hotspot. For instance, γ-TiAl alloys play an essential role in the development of aero-engines with a high thrust-weight ratio. These alloys have superior characteristics, including low density, high specific strength, significant creep resistance, and corrosion resistance in working temperatures of 500 ~ 850 ℃ [1-4]. However, further investigations showed that γ-TiAl alloys suffer from a potential safety hazard called “titanium fire” during the service at high temperatures. “Titanium fire” is an indirect accident in the aero-engine caused by the intense friction between rotor blades made of the titanium alloy and the casing after the deformation or breakage of rotor blades. Studies show that the risk of “titanium fire” limits the application of titanium alloys in aero-engines with a high thrust-weight ratio [5-7]. In order to inhibit high temperatures originating from the combustion in aero-engines, burn-resistant titanium alloys, and burn-resistant coatings have been developed for different applications in the aircraft industry.

The burn-resistant titanium alloys include T-Cr-V, Ti-Cu-Al, and Ti-Nb series. Ti-25V-15Cr-(2-3)Al alloys designed by Rolls-Royce have been applied to Trent series aero-engines and reduce burning risks in titanium alloy parts [8]. The BTT-1 (Ti-13Cu-4Al-4Mo-2Zr) and BTT-3 (Ti-18Cu-2Al-2Mo) alloys were developed from Ti-Cu eutectic alloys. Experiments showed that these alloys have significant burning resistance, while their poor fracture toughness and complex melting process limit their applications in aero-engine components [9,10]. Pratt and Whitney developed the Alloy C (Ti-35V-15Cr) and applied it to the F119-PW-100 aero-engine components. They showed that the yield and creep strengths of Alloy C at the working temperatures of 425~595 ℃ are superior to conventional titanium alloys, while it has

Corresponding author: weidongbo@nuaa.edu.cn[*]; lmfeng@nuaa.edu.cn[#];

https://doi.org/10.2298/JMMB200902005W

some defects such as poor processability and high manufacturing costs [11, 12]. The Ti40 (Ti-25V-15Cr-Si) and Ti14 (Ti-13Cu-1Al) β single-phase burn-resistant titanium alloys were designed by Northwest Institute for Non-ferrous Metal Research in China. However, these alloys are still in the laboratory stage and have poor processability and high manufacturing expenses [5, 7]. Currently, conventional burn-resistant titanium alloys cannot resolve the ignition and combustion problem of components made of titanium alloy.

On the other hand, studies show that the coating or surface alloying technologies can improve the hardness, wear-resistance, and erosion resistance of alloys. Moreover, these technologies can isolate titanium alloys from the ambient oxygen and heat, providing an effective method to inhibit the combustion of titanium alloys [13, 14]. Shen et al. [15] separately prepared Ti-Cr and Ti-Cu coating on the TC4 alloy by mechanical alloying and studied the burn-resistant performance of prepared samples. They proved that oxide layers of Cr and Cu retard the ignition by isolating the titanium alloy from the oxygen. Lou et al. [9] conducted an experimental study about the oxidation and combustion processes of Ti-Cu-NiCoAlTaY coating prepared on the TC4 alloy through the high-speed laser cladding technology. The combustion of TC4 alloy includes intense oxidation, ignition, and continuous combustion. Experiments showed that the coating has excellent heat dissipation and oxygen isolation properties, which may retard the combustion of TC4 alloy.

The booming design and manufacturing of aero-engines with a high thrust-weight ratio put forward higher requirements for titanium alloy components. Meanwhile, the two-layered ceramic coating is a promising approach to improve the performance of aero-engines [16, 17]. Generally, the two-layered ceramic coating consists of two layers, including an underlying bond coating and a top yttria-stabilized zirconia (YSZ) ceramic coating. It is worth noting that the top ceramic coating isolates the workpiece from the ambient environment and dissipates the heat, while the underlying bond coating consisting of Ni, Cr, Co, and Nb improves the bonding strength and the oxidation resistance [18,19]. Moreover, the composite structure reduces the thermal mismatch between the YSZ ceramic coating and the base material, thereby reducing the surface residual stress [18]. The two-layered ceramic coatings have been used in gas turbine components to improve their heat resistance and reduce the requirement for the cooling air.

The double glow (DG) plasma surface metallurgy technology is an innovative scheme for metal surface alloying based on ion nitriding and sputtering technology [20]. The DG technology requires lower processing temperatures compared with the conventional surface metallurgy technology, thereby reducing impacts on the dimension and microstructure of the base material and increasing the metallurgical bonding between the coating layer and the base material [21, 22]. Reviewing the literature indicates that the surface co-alloying of Ni-Cr through the DG technology remarkably improves the high-temperature oxidation resistance of TC4 alloy, while the addition of Ni can further enhance the adhesion of alloy coating [23]. Studies show that the Ni-Cr alloy coating has excellent high-temperature oxidation resistance and similar thermal expansion coefficient to γ-TiAl alloy, which makes it an appropriate choice as the bond coating [18, 19, 24]. Zhang et al. [20] applied the double glow plasma metallurgy technology and fabricated Ti-Cr coating upon the Ti-6.5Al-0.3Mo-1.5Zr-0.25Si titanium alloy. They proved that the fabricated coating retards the combustion of the substrate alloy unless it is peeled off.

Recently, the multi-arc ion plating (MAIP) has achieved industrial production. This scheme utilizes the arc discharge to evaporate and ionize the alloy target and deposit alloy coating on the specimen surface. In this method, the alloy target is simultaneously vaporized through multiple arcs thereby significantly improving the coating efficiency. On the other hand, the interfacial inter-diffusion of atoms reduces the internal stress and increases the bonding strength of the coating. MAIP provides a low-cost and highly efficient production way for the preparation of alloy coatings, which also realizes the fabrication of ceramic coating [25, 26].

Although the two-layered ceramic coating has wide application prospects in raising the working temperature of aero-engine parts, only a few investigations have been conducted on this issue so far. Considering this shortcoming, the main purpose of the present study is to investigate the performance of NiCr/YSZ coating fabricated on γ-TiAl alloy. To this end, it is intended to prepare an underlying Ni-Cr bond coating and a top YSZ ceramic coating through DG and MAIP technologies, respectively. Moreover, the bonding strength of the NiCr/YSZ coating will be tested by thermal shock tests, while the corresponding burn resistance will be evaluated through the laser spot melting test.

2. Experimental details

2.1. Materials and methods

The substrate material used in this experiment was γ-TiAl alloy with the chemical composition of 46.5 Al, ≤1.5 V, ≤1 Cr, ≤0.2 Nb, ≤0.1 C, ≤0.05 N, ≤0.015 O and balance Ti (wt.%). The specimens (14 mm × 14 mm × 5 mm) were ground with SiC paper and

polished to 1000 grit, and then ultrasonically cleaned before coating preparation.

Herein, the Ni-Cr bond coating was prepared on the surface of γ-TiAl alloy by DG technology using the Cr20-Ni80 (wt.%) alloy target. The argon was used as working atmosphere. The corresponding experimental parameters are shown in Table 1. The YSZ ceramic coating was prepared as top coating by MAIP technology using the cylindrical Zr92-Y8 (wt.%) alloy target. The oxygen was used as the working atmosphere and argon was used as protective atmosphere. The corresponding experimental parameters are shown in Table 2.

Table 1. *Processing parameters of plasma Ni-Cr alloying*

Voltage of the source / V	Voltage of the substrate / V	Working pressure / Pa	Distance between target and specimen / mm	Time / h
900	560	40	18	3

Table 2. *Processing parameters of ion plating YSZ coating*

Flow rate of oxygen / sccm	Flow rate of argon / sccm	Negative bias / V	Arc current / A	Pressure / Pa	Temp-erature / ℃	Time / h
10	100	200	100	0.3Pa	350	1.5

2.2. Microstructure characterization

The surface morphology, cross-section morphology, and chemical compositions of NiCr/YSZ coating were characterized by a HITACHI S-4800 scanning electron microscope (SEM) equipped with energy dispersive X-ray spectroscope (EDS). The surface phase identification of NiCr/YSZ coating was performed by D/Max 2500 X-ray diffraction (XRD) with CuKα radiation over arrange of 2θ from 10° to 90°.

2.3. Microhardness and bonding strength test

The microhardness of γ-TiAl alloy and NiCr/YSZ coating were separately measured by HXS-1000A microhardness tester at the load of 0.1 kgf and holding for 10 s. The measurement points were selected along the diagonal of the specimen with an interval of 2 mm. The surface strengthening effect of NiCr/YSZ coating was characterized by analyzing the average microhardness of the composite coating and γ-TiAl substrate.

The violent temperature fluctuations of aero-engine components always lead to surface structural trauma. The failure occurs when the strain caused by the surface coating expanding or contracting at a different rate than substrate alloy exceeds the tensile strength of the surface coating. Therefore, the thermal shock test is suitable for evaluating the bonding strength of NiCr/YSZ coating. The experiment steps were as follows. Firstly, the muffle furnace was heated to 1000 ℃ at a rate of 20℃/min. The specimens were put into porcelain crucibles in the furnace chamber and hold for 15 minutes. Subsequently, the specimens were taken out and quenched into cool water. The specimens were heated and cooled continuously until the peeled off area of coating reached about 5%, and recorded the repetitions. The bonding strength of NiCr/YSZ coating after thermal shock test was evaluated by analyzing the surface morphology, cross-section morphology, and chemical compositions of the coating.

2.4. Laser spot melting test

The methods for testing and evaluating the burn resistance of titanium alloys mainly include equal friction method, metal droplet method, direct-current simulation burning method, and laser spot melting method [5, 15]. The laser spot melting can control multiple parameters and intuitively characterize the burn resistance of materials. In this study, the burn resistance of γ-TiAl alloy with NiCr/YSZ coating was preliminarily evaluated by laser spot melting test. Prior to the test, the specimen surface was cleaned by ultrasonic cleaner. The specimens were irradiated by laser beam at the exposure time of 200 ms and the power of 300~1200 W. The distance of specimens and laser heat source was 200 mm.

3. Results and discussion

3.1. Microstructure and composition of NiCr/YSZ coating

Figure 1 illustrates the surface morphology, chemical composition, and phase distribution of the NiCr/YSZ coating. It is observed that the coating is dense and has no cracks and porosities. Moreover, it is found that some scattered metal droplets are attached to the depression. These droplets are formed during the fabrication of YSZ ceramic coating by the MAIP technology. The target metal is bombarded by ions to form a molten pool. When positive ions return to the cathode, the flow of metal vapor in the micro-melting pool and the bombardment bring metal droplets to the coating surface. It should be indicated that the ionization rate can be raised to reduce metal droplets through adjusting the bias voltage and the magnetic field distribution. The YSZ ceramic coating consists of O, Y and Zr, where the weight ratio of Zr to Y elements is 78.21:21.79. Compared with the weight

ratio 92:8 of the alloy target, the proportion of Y is high, which originates from its higher sputtering and deposition rate. Figure 1d presents XRD patterns of NiCr/YSZ coating. The YSZ ceramic coating mainly consists of ZrO_2. The weakly diffraction peaks of Zr and Y_2O_3 in the XRD patterns indicate that the YSZ ceramic coating may contain a trace amount of Zr and Y_2O_3 oxide.

Figure 2 shows the cross-section morphology and elements distribution of the NiCr/YSZ coating. The coating exhibits a duplex structure that is tightly adhered to the substrate, without inclusions or porosities. Figure 2b shows the EDS results of the NiCr/YSZ coating. It should be indicated that the top YSZ ceramic coating is composed of Zr, Y and O, and the underlying bond coating consists of Ni and Cr. Moreover, the thickness of the NiCr/YSZ coating is approximately 19 μm, including 12 μm YSZ ceramic coating (zone I) and 7 μm Ni-Cr bond coating (zone II deposited layer and III interdiffusion layer). It is worth noting that the continuous gradient transition of elements in the interface is beneficial to the bonding strength.

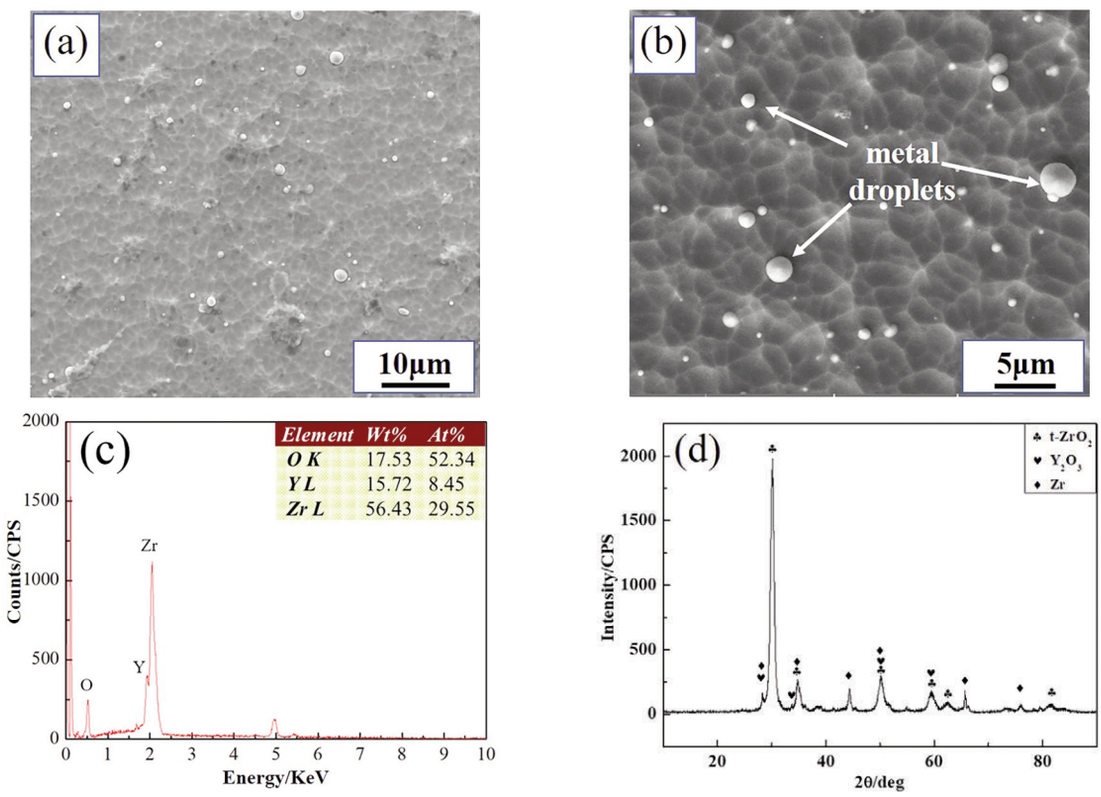

Figure 1. *Surface morphology and chemical composition of NiCr/YSZ coating (a) (b) surface morphology (c) elemental composition (d) phase composition*

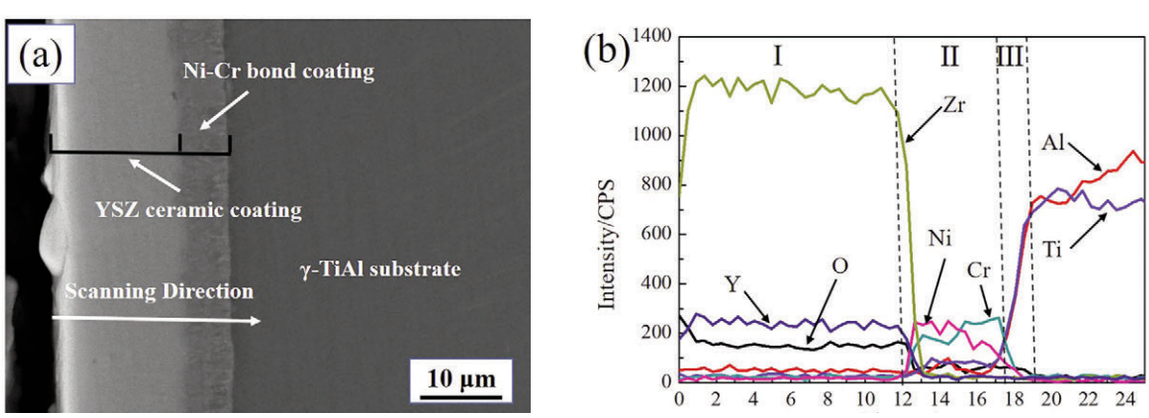

Figure 2. *Cross-section morphology and elements distribution of γ-TiAl substrate coated with NiCr/YSZ coatings (a) cross-sectional morphology (b) elements distribution*

3.2. Microhardness and bonding strength

Figure 3 shows the microhardness comparison between the γ-TiAl substrate and the NiCr/YSZ coating. It is observed that the microhardness of the γ-TiAl substrate is between 277.4~333.7 $HV_{0.1}$, with an average value of 299.7 $HV_{0.1}$. Moreover, the microhardness of the NiCr/YSZ coating is between 806.7~915.2 $HV_{0.1}$, with an average value of 872.6 $HV_{0.1}$. The average microhardness of NiCr/YSZ coating is raised by a factor of about 2 compared to the γ-TiAl substrate. The microhardness standard deviation of the NiCr/YSZ coating is 85.38 $HV_{0.1}$. Therefore, the surface hardness of the NiCr/YSZ coating is more homogeneous. The NiCr/YSZ coating significantly improves the surface hardness of the γ-TiAl substrate.

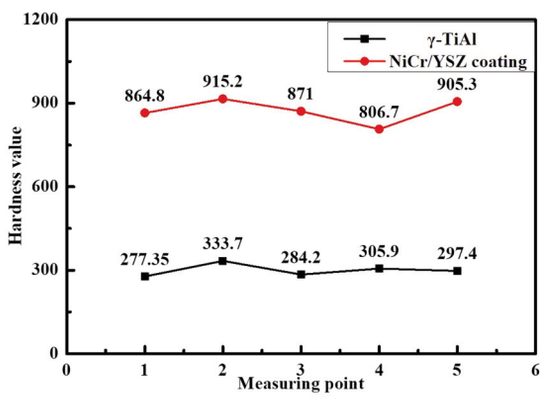

Figure 3. *Microhardness of γ-TiAl and NiCr/YSZ coating*

The aero-engine components always undergo violent temperature fluctuations during service. The thermal shock resistance is a reasonable indicator to evaluate the bonding strength of the NiCr/YSZ coating [16, 27]. Figure 4 illustrates the failure process of the NiCr/YSZ coating during the thermal shock test. In the fifth experiment, the microcracks initially appear on the metal droplets. With the continuous heating and cooling, the residual stress caused by the volume expansion after the oxidation of metal droplets exceeds the tensile strength of the material, leading to cracks initiation and expansion. As the experiment proceeds, the cracks continuously develop on the coating surface, and the length of cracks reaches about 10 μm at the 30th test. At the 40th test, the ceramic coating gradually cracks and partly peels off. Moreover, the cracks gradually expand longitudinally and provide a channel for the oxygen to impregnate inward. Finally, at the 48th test, the peeling area reaches about 5% of the coating, thereby the coating is failed.

Figure 5 shows the cross-section morphology and elements distribution of NiCr/YSZ coatings with

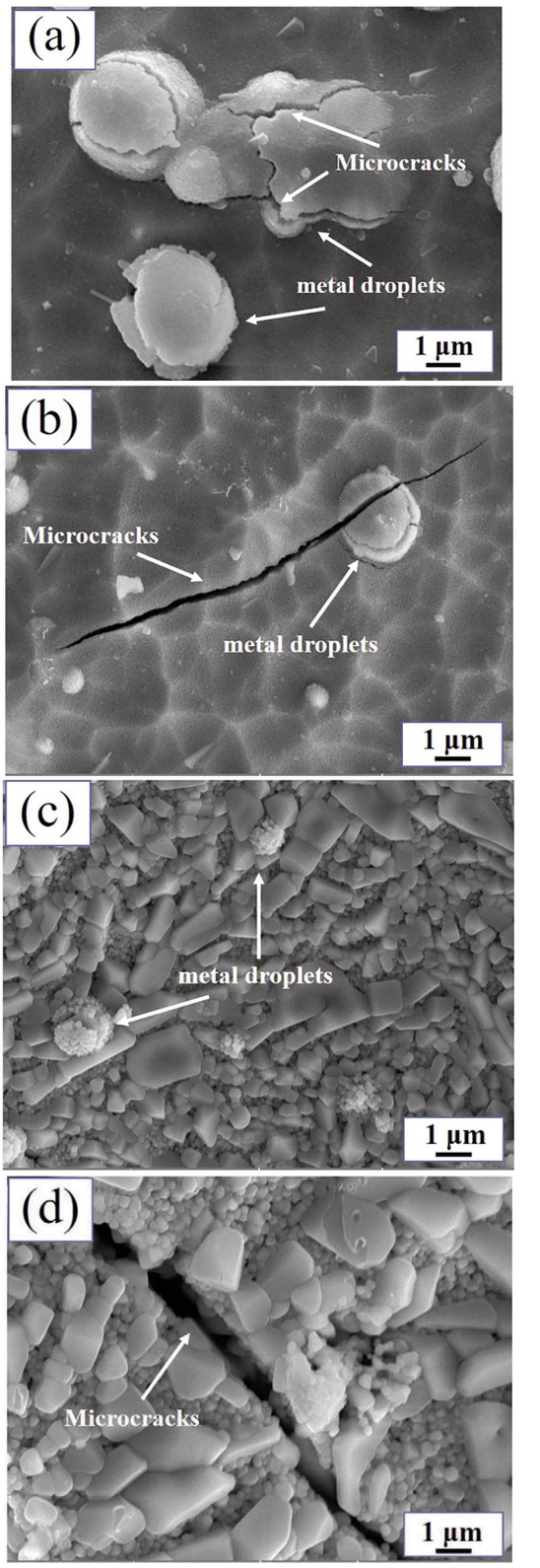

Figure 4. *Surface morphology of NiCr/YSZ coating with different thermal shock times (a) 5th (b) 30th (c) 40th (d) 48th*

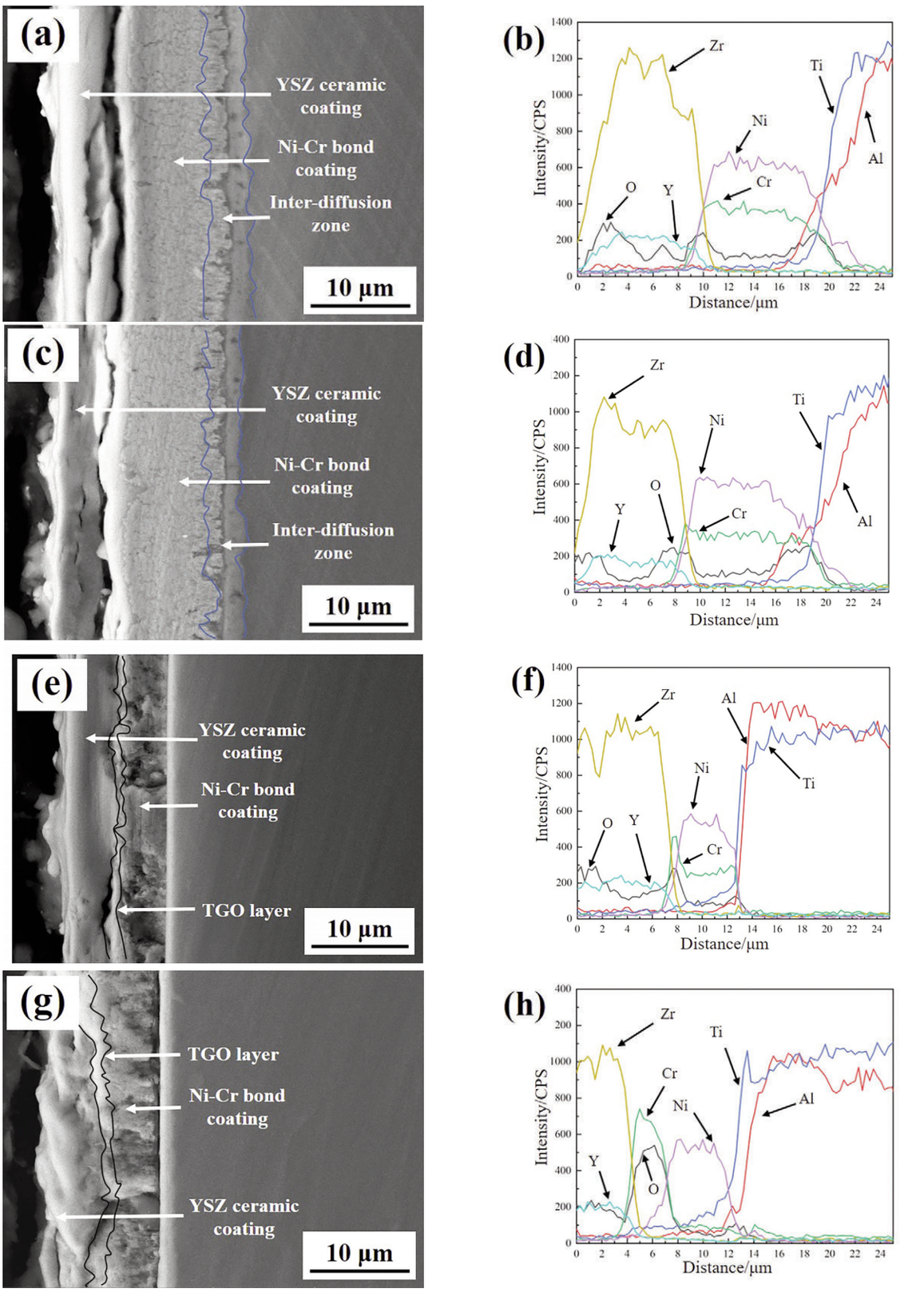

Figure 5. *Cross-section morphology and elements distribution of NiCr/YSZ coatings with different thermal shock times (a)(b) 5th (c)(d) 30th (e)(f) 40th (g)(h) 48th*

different thermal shock times. In the 5^{th} ~ 30^{th} experiments, the coating retains the original structure, which consists of the top YSZ ceramic coating and the underlying Ni-Cr bond coating. Figure 5b and 5d illustrate that the content of O on the surface increases significantly, indicating that the oxidation of YSZ ceramic coating occurs on the surface metal droplets during the thermal shock test. It should be indicated that the interdiffusion layer of Ni, Cr, Ti and Al at the interface of the Ni-Cr bond coating and the γ-TiAl substrate is approximately 6 ~ 7 μm (Fig. 2) the interdiffusion layer in the preparation is about 3 μm, which may be due to the inter-diffusion of coating elements and the γ-TiAl substrate elements at high temperature. In the 40^{th} ~ 48^{th} experiments, the thickness of the coating decreases significantly due to the cracking and peeling after thermal shock test. The content of O and Cr increase significantly at the interface of YSZ ceramic coating and Ni-Cr bond coating, indicating that a TGO layer dominated by Cr oxides form at the interface and grows continuously.

The thermal shock test denotes that the microcracks initially form on the surface defects such as metal droplets. This highlights the importance of the coating surface quality. As the dimension of cracks increases, the oxygen invades the YSZ coating and contacts the underlying Ni-Cr alloy coating to form a TGO layer dominated by Cr oxide. Moreover, the structure of the oxide layer is an important factor for the bonding strength of the YSZ coating [16, 24]. Therefore, the growth rate of microcracks and oxidized layer determines the bonding strength of the YSZ ceramic coating. It should be indicated that the Ni-Cr alloy coating prepared by the DG technology possesses excellent oxidation resistance, which retards the growth of TGO layer and improves the bonding strength of the YSZ coating. During the test, the mutual diffusion of elements occurs at the interface between the Ni-Cr bond coating and the γ-TiAl substrate, forming the inter-diffusion zone. The atomic vacancies and the second phase formed in in the inter-diffusion zone weaken the stability of the coating, while the composition gradient formed by the inter-diffusion enhances the adhesion between the coating and the γ-TiAl substrate [28]. The composite structure of the NiCr/YSZ realizes the improvement of the bonding strength between the YSZ ceramic coating and the γ-TiAl substrate.

3.3. Burn resistant properties

In order to evaluate the burn resistance of the NiCr/YSZ coating coated on the γ-TiAl substrate, the laser spot melting test is carried out on the γ-TiAl alloy and NiCr/YSZ coating coated on the γ-TiAl substrate at the irradiation powers of 300 W, 600 W, 1000 W, and 1200 W. The burning behaviors of the γ-TiAl alloy and NiCr/YSZ coating are studied in detail by analyzing the surface morphology, elemental composition and surface profile.

Figure 6 shows the surface morphology and elemental composition of the γ-TiAl alloy after the laser spot melting test. At the power of 300 W, the microcracks appear in the center of the ablation zone. When the irradiation power reaches 600 W, the specimen rapidly melts and solidifies to form the re-solidification zone. The ablation zone exhibits petal-like combustion products and some macro cracks. When the irradiation power exceeds 1000 W, the petal-like combustion products are gradually replaced by conical combustion products due to the more violent ablation process. It is observed that lots of scattered residues are formed around the ablation zone, indicating that the specimens are evaporated and destroyed severely. The surface ablation morphology indicates that the ablation area and crack size gradually expand as the irradiation power increases. When the heating temperature exceeds the melting point of the γ-TiAl alloy, the melting and evaporation can absorb some combustion heat, which partly weakens its combustion ability. The EDS results show that the ablation zone consists of Ti, Al, V and O. As the irradiation power increases, the oxygen content in the ablation zone decreases from 7.80% (at%) to 2%~3%, indicating that some oxides may be sputtered to the edge zone. Moreover, there is no dense oxide layer formed on the γ-TiAl substrate. Therefore, the laser beam directly destroys the surface structure of the γ-TiAl substrate.

Figure 7 shows the surface morphology and elemental composition of the NiCr/YSZ coating after the laser spot melting test. At the power of 300 W, some ablation scars and spots are formed in the ablation zone, while the YSZ ceramic coating remains intact. When the irradiation power increases to 600 W, an ablation pit and several microcracks appear on the coating surface, while the YSZ ceramic coating still covers the ablation zone. When the irradiation power exceeds 1000 W, the YSZ ceramic coating is destroyed and the area of the ablation pit increases significantly. Moreover, the specimen materials are partly sputtered into the surrounding zone, forming some scattered residues. The surface ablation morphology indicates that the YSZ ceramic coating is not melted and evaporated due to its higher melting point. Therefore, it can partially isolate and dissipate the heat to reduce the ablative damage. However, as the heating temperature increases, the NiCr/YSZ coating is gradually destroyed, weakening its protective ability. Furthermore, the EDS results show that the surface elements mainly consist of Zr, O, Y, Ti, Al, Ni, and Cr. Due to the destruction of the composite ceramic coating, Ti, Al, Ni, and Cr are detected in the ablation zone. As the power increases,

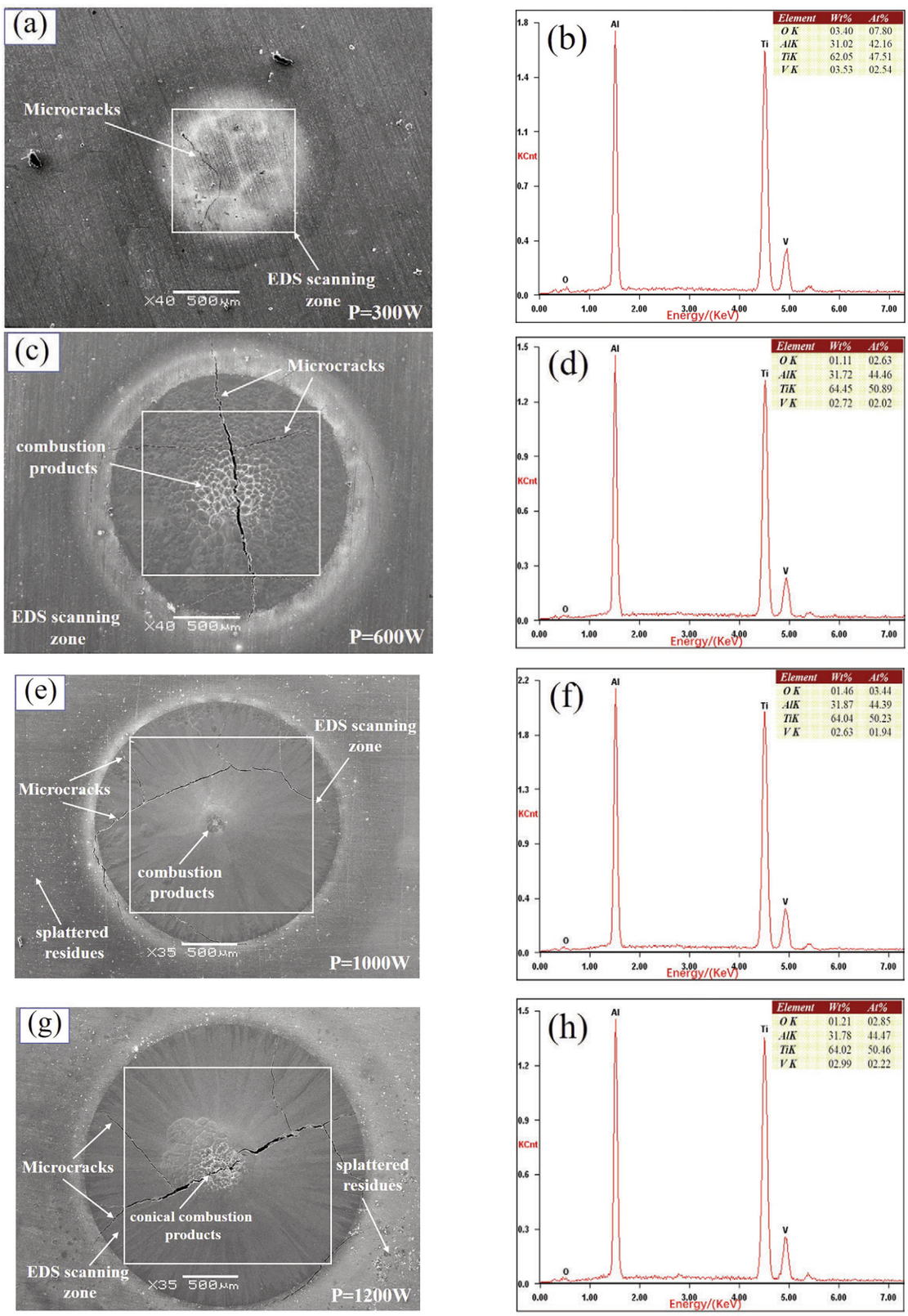

Figure 6. *Surface morphology and elemental composition of γ-TiAl alloy after laser spot melting at different irradiation powers (a) (c) (e) (g) surface morphology; (b) (d) (f) (h) elemental composition*

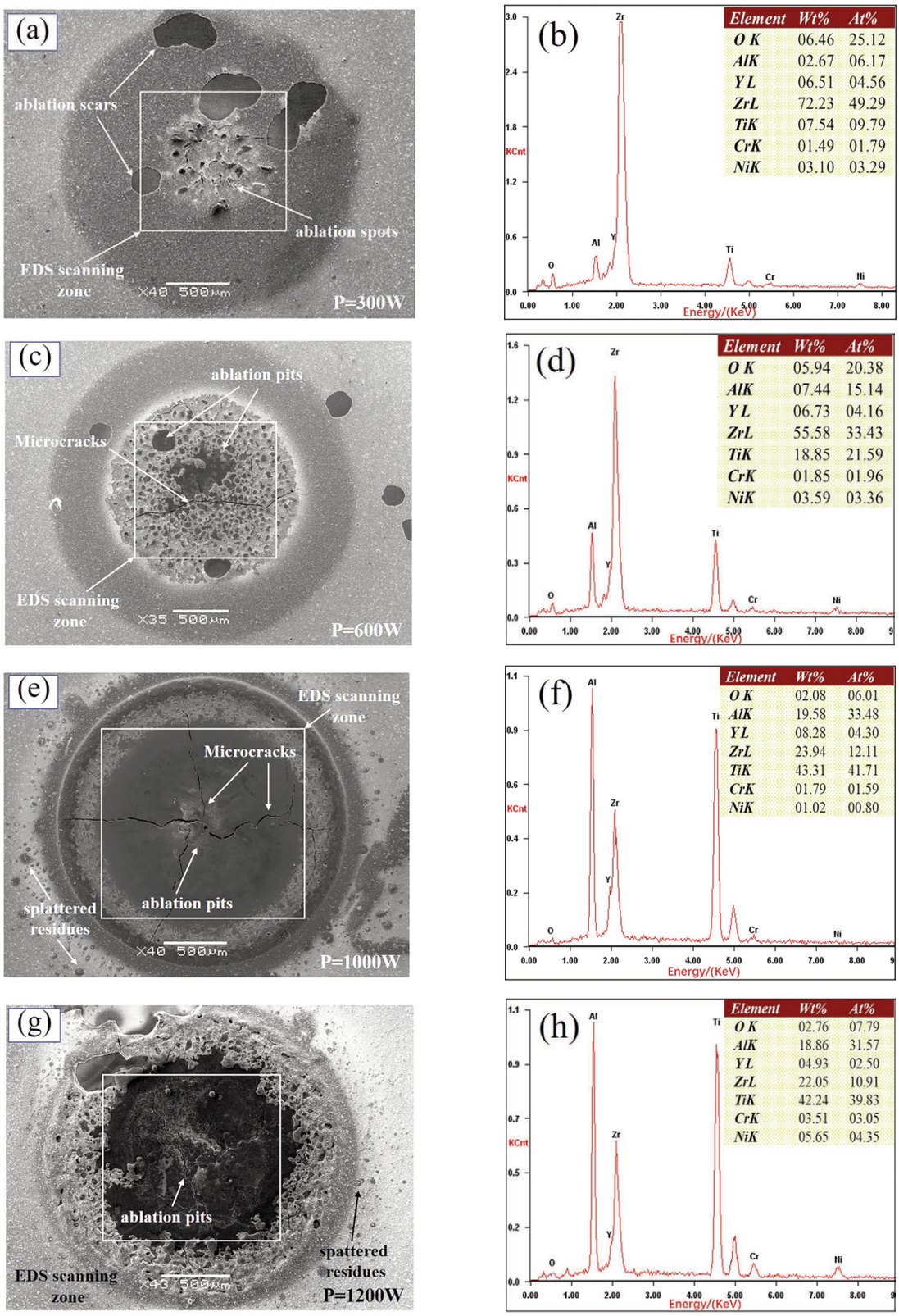

Figure 7. *Surface morphology and elemental composition of NiCr/YSZ coatings after laser spot melting at different irradiation powers (a) (c) (e) (g) surface morphology; (b) (d) (f) (h) elemental composition*

the elemental content proportion of Zr, O, and Y gradually decreases, indicating that the structure of the composite ceramic coating is further damaged. Under the protection of the NiCr/YSZ coating, the ablation effect is not completely removed, while the damage is partly compensated.

Figure 8 shows the surface profile of the γ-TiAl substrate. Moreover, Table 3 presents the dimensions of the ablation zone. The γ-TiAl substrate melts and solidifies rapidly to form raised combustion products after the laser ablation. Since the heat source of the laser beam is a Gaussian distributed heat resource, the laser energy density reaches the maximum value in the center of the ablation zone. Therefore, the ablation damage in the center zone is significant [9]. As the irradiation power increases, the ablation zone expands and the height of combustion products increases gradually. Moreover, the diameter of the ablation zone and the height of combustion products increase from 2.0 mm to 2.6 mm and from 3.5 μm to 100 μm, respectively. The dimensions are estimations rather than precise values. When the irradiation power is above 1000 W, the combustion products are accumulated to form a conical protrusion. Moreover, the ring-shaped ablation pit is formed around the combustion products. The height of combustion products dramatically increases, indicating that specimens undergo serious ablation. Figure 8g shows that the combustion products are collapsed when the irradiation power reaches 1200 W

Table 3. *The ablation zone dimension of γ-TiAl*

Irradiation power (W)	300	600	1000	1200
Ablation diameter (mm)	2	2	2.2	2.6
Combustion products height (μm)	3.5	17.5	100	89

Figure 9 shows the surface profile of NiCr/YSZ coating. Moreover, Table 4 presents the dimensions of the ablation zone. Different from the ablation behavior of the γ-TiAl substrate, the NiCr/YSZ coating can partly alleviate the ablation damage through heat insulation and heat dissipation. As the heating temperature increases, the ceramic coating in the center of the ablation zone is gradually destroyed. Then, the ablation pit is left in the center and the scattered residues are formed around the ablation zone. Moreover, the central heat source diffuses outwards, heating the surrounding ceramic coating and forming the protruding combustion products around the ablation pit. As the irradiation power increases, the area of the ablation zone and the depth of the ablation pit do not increase significantly. The diameter and the depth of the ablation pit increase from 1.5 mm to 1.8 mm and from 11.5 μm to 18.5 μm, respectively. The volume change of the ablation pit surface shows that the ablation destruction does not increase significantly as the irradiation power increases. Under the same irradiation power, the diameter of the ablation zone and the height of the ablation product on NiCr/YSZ coating are noticeably smaller than those in the γ-TiAl substrate. Moreover, the maximum depth of the ablation pit is close to the thickness of the composite coating, indicating that the coating retards the ablation process and protects the γ-TiAl substrate. The ablation range is effectively controlled.

Table 4. *The ablation zone dimension of NiCr/YSZ coating*

Irradiation power (W)	300	600	1000	1200
Ablation zone diameter (mm)	1.5	1.7	1.8	1.7
Ablation pit depth (μm)	11.5	11.5	13	18.5

As the irradiation power increases, the ablation of the specimens becomes more serious. The burn resistant effects of the NiCr/YSZ coating on the γ-TiAl alloy are illustrated by studying their combustion behaviors at different heat inputs. The combustion process of titanium alloys includes the rapid oxidation, ignition, and continuous combustion [9]. The oxygen, heat and fuel are necessary to maintain the combustion process. Therefore, reducing one of these factors can retard the combustion of titanium alloys [5, 15].

The γ-TiAl alloy tends to form the non-protective TiO_2-enriched oxide layer, which cannot prevent the transmission of oxygen and heat. Therefore, due to the lack of protection, the γ-TiAl alloy is directly exposed to the high-energy laser beam during the laser spot melting test. Figure 6 shows that when the irradiation power exceeds 600 W, severe ablation occurs on the specimen surface. Moreover, no dense and continuous oxide layer is formed in the ablation zone. When the combustion temperature exceeds the melting points of the γ-TiAl alloy, the ablation zone melts to form the conical combustion products and a part of the material is sputtered into the surrounding zone.

The ablation behavior of the NiCr/YSZ coating is different from that of the γ-TiAl substrate. Moreover, the melting point of the YSZ ceramic coating is higher than that of the γ-TiAl substrate, which increases the heat resistance of γ-TiAl alloys. The dense YSZ ceramic coating provides an insulating barrier to prevent heat conduction, dissipate heat and isolate the oxygen in the environment, thereby retarding the

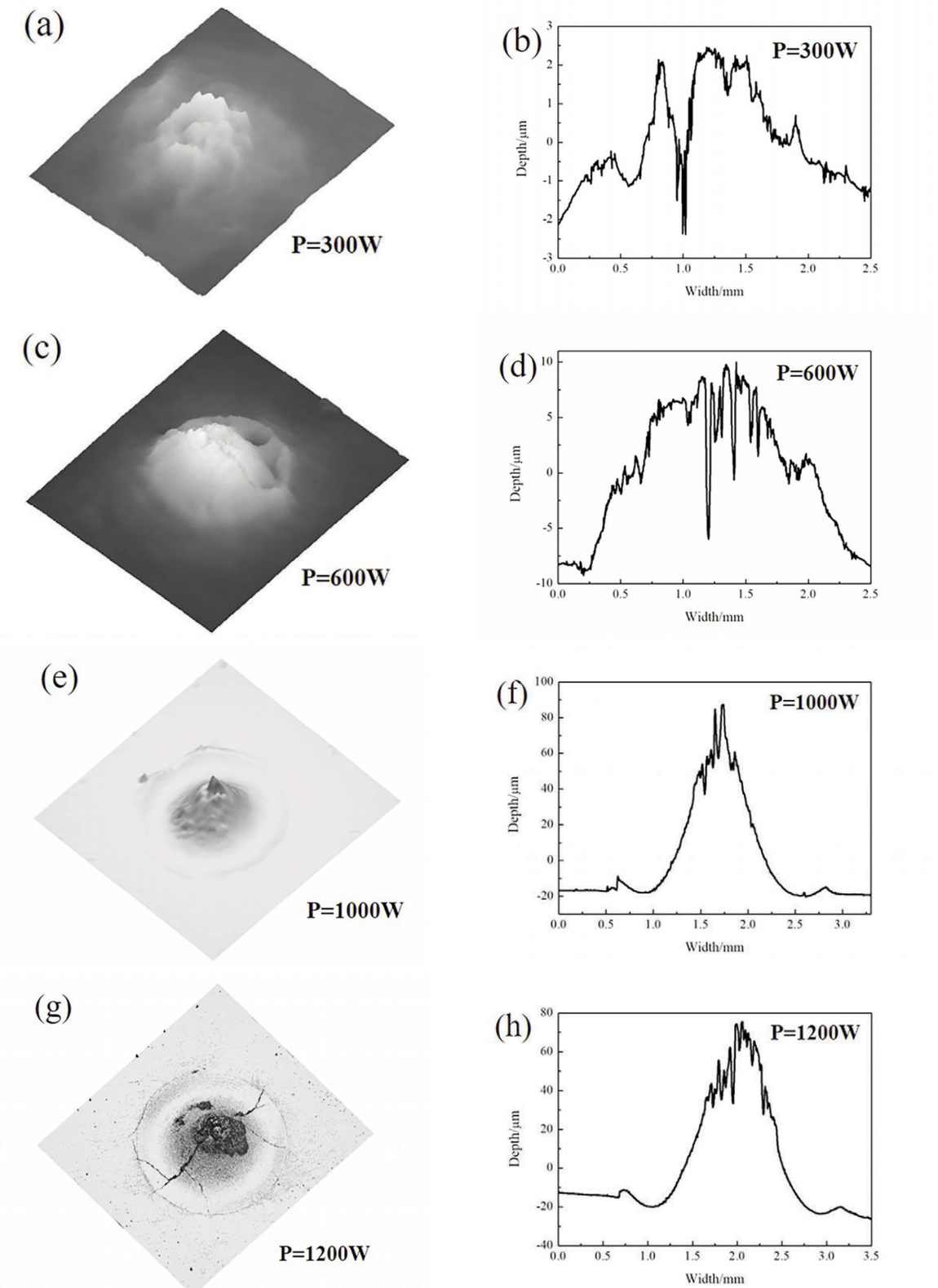

Figure 8. *The surface profile of γ-TiAl alloy after laser spot melting at different irradiation powers (a) (c) (e) (g) Three-dimensional ablation morphology; (b) (d) (f) (h) surface profile*

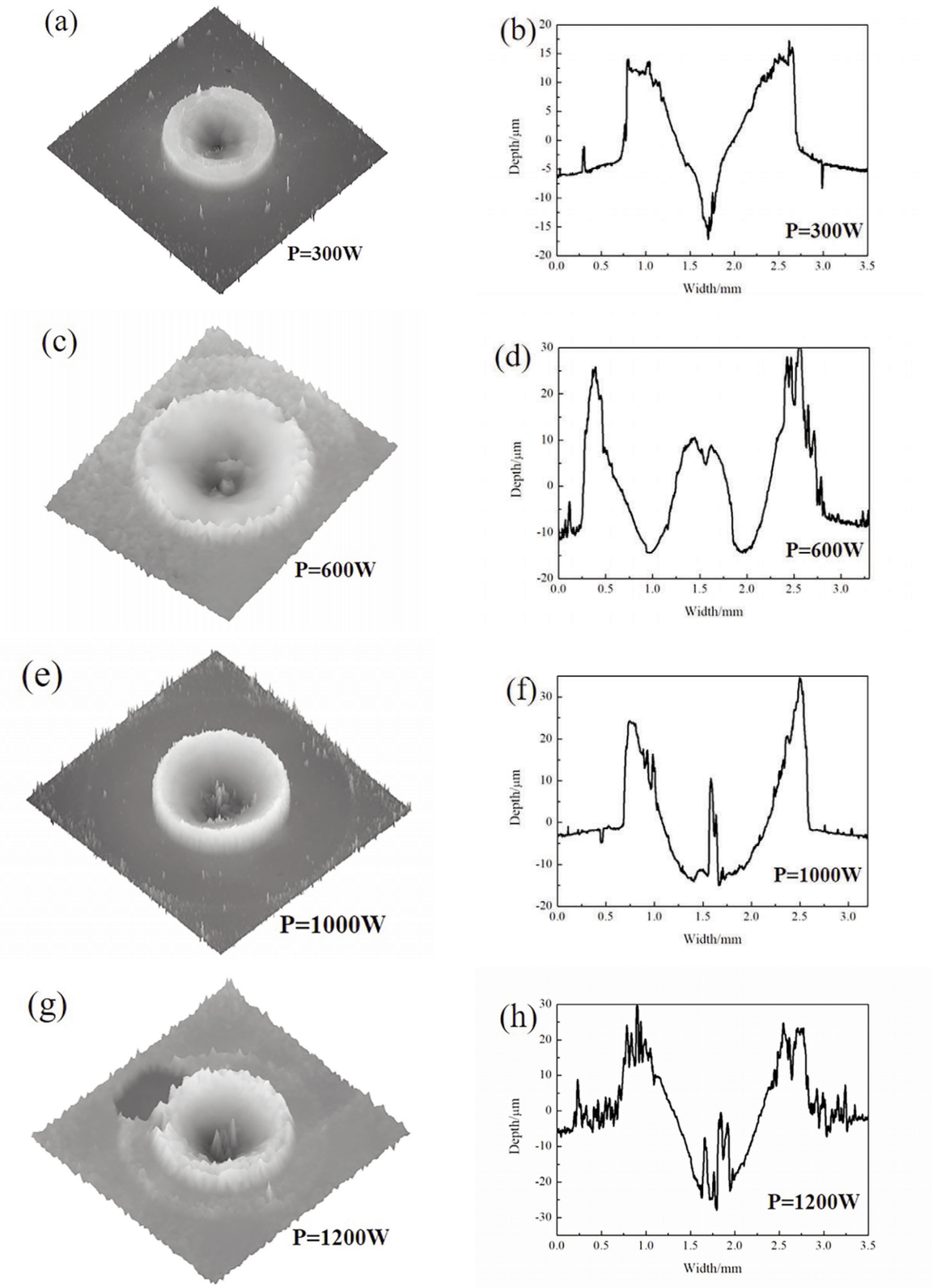

Figure 9. *The surface profile of NiCr/YSZ coating after laser spot melting at different irradiation powers (a) (c) (e) (g) Three-dimensional ablation morphology; (b) (d) (f) (h) surface profile*

combustion process [18]. It is worth noting that the Ni-Cr alloy coating has excellent oxidation resistance. When NiCr/YSZ coating is exposed to oxygen at high temperature, the dense mixed oxide layer of NiO and Cr_2O_3 formed on the interface can also prevent oxygen from invading, thereby preventing the further expansion of the combustion [23,24]. Figure 7 illustrates the surface ablation morphology and EDS results, which exhibit the ablation extent of NiCr/YSZ coating under different irradiation powers. When the irradiation power is below 600 W, the coating structure is slightly destroyed by the laser beam. Meanwhile, when the irradiation power exceeds 1000 W, the element content of Ti and Al exceeds the coating elements, indicating that the NiCr/YSZ coating is further destroyed. Figure 8 shows that the γ-TiAl substrate exposed at the center of the ablation pit melts to form a conical combustion product of about 15 μm. However, the NiCr/YSZ coating controls the ablation range within 1.8 mm and reduces the ablation damage under the same heat input.

Both γ-TiAl alloys and NiCr/YSZ coating can be ignited by the laser beam when the heat input reaches an appropriate level. The NiCr/YSZ coating possesses better heat resistance. Therefore, the probability of the specimens being ignited is reduced when the radiant energy is absorbed by the alloy coating. The heat insulation and heat dissipation of the alloy coating also retard the combustion process. If the ablation is slight, the complete structure of the NiCr/YSZ coating can inhibit the invasion of the oxygen to resolve the possibility of combustion. It is found that the NiCr/YSZ coating improves the burn resistance of γ-TiAl alloys.

4. Conclusions

(1) The NiCr/YSZ coating was fabricated on γ-TiAl substrate by combining double glow plasma surface metallurgy technology and multi-arc ion plating technology. The coating was dense and homogeneous, without cracks, holes and inclusions.

(2) The average microhardness of NiCr/YSZ coating was raised by a factor of about 2 compared to the γ-TiAl substrate. The thermal shock test indicated that the composite structure of the NiCr/YSZ realized the improvement of the bonding strength between the YSZ ceramic coating and the γ-TiAl substrate. The continually expanded cracks provided a channel for oxygen invading, while the Ni-Cr alloy coating retarded the further oxidation.

(3) The γ-TiAl alloy underwent serious ablation after the laser spot melting test due to its poor burn resistance. The NiCr/YSZ coating retarded the combustion process through insulating and dissipating heat. Under the protection of NiCr/YSZ coating, no intense burning occurred on the surface of specimens and the ablation damage was obviously decreased, which reduced the risk of "titanium fire".

Acknowledgments

Natural Science Foundation supported this project for Excellent Young Scientists of Jiangsu Province, China (Grant No. BK20180068), Opening Project of Materials Preparation and Protection for Harsh Environment Key Laboratory of Ministry of Industry and Information Technology (Grant No. XCA20013-1), Opening Project of Aero-engine Thermal Environment and Structure Key Laboratory of Ministry of Industry and Information Technology, China (Grant No. CEPE2019005).

Reference

[1] M. Perrut, P. Caron, M. Thomas, A. Couret, C. R. Phys., 19 (8) (2018) 657-671.

[2] H.W. Liu, Z.X. Li, F. Gao, Y.G. Liu, Q.F. Wang. J. Alloys Compd., 698 (2017) 898-905.

[3] P.X. Ouyang, G.B. Mi, J.X. Cao, X. Huang, L.J. He, P.J. Li, Mater. Today Commun., 16 (2018) 364-373.

[4] S.W. Kim, J.K. Hong, Y.S. Na, J.T. Yeom, S.E. Kim, Mater. Des., 54 (2014) 814-819.

[5] Y.N. Chen, Y.Z. Huo, X.D. Song, Z.Z. Bi, Y. Gao, Y.Q. Zhao, Int. J. Miner. Metall. Mater., 23 (02) (2016) 215-221.

[6] H. Clemens, S. Mayer, Mater. High Temp., 33 (4-5) (2016) 1-11.

[7] G.B. Mi, X. Huang, J.X. Cao, C.X. Cao, X.S. Huang, Trans. Nonferrous Met. Soc. China, 23 (08) (2013) 2270-2275.

[8] X. Wu, R. Sharman, J. Mei, W. Voice, Mater. Des., 23 (3) (2002) 239-247.

[9] L.Y. Luo, Y. Zhang, Y.J. Jia, Y. Li, H.F. Tian, Y.J. Cai, C.X. Li, Surf. Coat. Technol., 392 (2020) 125697.

[10] Y.Q. Zhao, X.M. Zhao, K.Y. Zhu, G.Z. Luo, L. Zhou, Rare Metal Mat. Eng., 25 (5) (1996) 3-8.

[11] A.K. Gogia, Def. Sci. J., 55 (2) (2005) 149-173.

[12] J. Paul, Ph. D Bania, JOM, 46 (7) (1994) 16-19.

[13] R.R. Boyer, Mater. Sci. Eng., A, 213 (1-2) (1996) 103-114.

[14] J.P. Merutka, Am. Ceram. Soc. Bull., 59 (1980) 604-621.

[15] B. Li, R.D. Ding, Y.F. Shen, Y.Z. Hu, Y. Guo, Mater. Des., 35 (2012) 25-36.

[16] Q.M. Liu, S.Z. Huang, A.J. He, J. Mater. Sci. Technol., 35 (12) (2019) 2814-2823.

[17] R. Darolia, Int. Mater. Rev., 58 (6) (2013) 315-348.

[18] C.X. Pan, X.R. Xu, Surf. Coat. Technol., 162 (2-3) (2003) 194-201.

[19] S. Nouri, S. Sahmani, M. Asayesh, M.M. Aghdam, Intermetallics, 118 (2020) 106704.

[20] P.Z. Zhang, Z. Xu, G.H. Zhang, Z.Y. He, Surf. Coat. Technol., 201 (9-11) (2007) 4884-4887.

[21] D.B. Wei, P.Z. Zhang, Z.J. Yao, J.T. Zhou, X.F. Wei, X.H. Chen, Vacuum, 121 (2015) 81-87.

[22] D.B. Wei, P.Z. Zhang, Z.J. Yao, X.H. Chen, F.K. Li, Vacuum, 155 (2018) 233-241.

[23] D.B. Wei, P.Z. Zhang, Z.J. Yao, X.F. Wei, J.T. Zhou, X.H. Chen, Appl. Surf. Sci., 388 A (2016) 571-578.

[24] L.R. Luo, X. Shan, Z.H. Zhou, C.S. Zhao, X. Wang, A.P. Zhang, X.F. Zhao, F.W. Guo, P. Xiao, Corros. Sci., 126 (2017) 356-365.

[25] L. Wang, S.H. Zhang, Z. Chen, J.L. Li, M.X. Li, Appl. Surf. Sci., 258 (8) (2012) 3629-3636.

[26] X.Y. Guan, Y.X. Wang, G.G. Zhang, X. Jiang, L.P. Wang, Q.J. Xue, Tribol. Int., 106 (2017) 78-87.

[27] R.Z. Wang, W.G. Li, D.Y. Li, X.L. Shen, X.B. Zhang, B. Li, J.Y. Yao, X.Z. Wu, D.N. Fang, J. Alloys Compd., 626 (2015) 56-59.

[28] H.R. Yao, C.Y. Jiang, Z.B. Bao, S.L. Zhu, F.H. Wang, J. Mater. Eng. Perform., 28 (2019) 1019-1029.

PRIPREMA NiCr/YSZ DVOSLOJNOG PREMAZA OTPORNOG NA TOPLOTU ZASNOVANA NA METODAMA POVRŠINSKE OBRADE UPOTREBOM PLAZME I JONSKOG OBLAGANJA

D.-B. Wei [a,b,*], M.-F. Li [a,b,#], X. Zhou [a,b], F.-K. Li [a,b], S.-Q. Li [a,b], P.-Z. Zhang [a,b]

[a] Fakultet za nauku o materijalima i tehnologiju,
Univerzitet za aeronautiku i astronautiku u Nanđingu, Nanđing, Kina.
[b] Glavna laboratorija za pripremu i zaštitu materijala koji se koriste u surovim uslovima Ministarstva industrije i informacione tehnologije, Nanđing, Kina

Apstrakt

NiCr/YSZ premaz je izrađen na γ-TiAl leguri uz pomoć dvostruko tretirane obrade površine upotrebom plazme i tehnologijom višestruko lučnog jonskog oblaganja. Detaljno su ispitani mikrostruktura, mikrotvrdoća, čvrstoća prijanjanja kao i otpornost NiCr/YSZ premaza na toplotu. Rezultati su pokazali da je NiCr/YSZ premaz čvrst i homogen, uključujući i dupleksnu strukturu površinskog YSZ keramičkog premaza i osnovnog Ni-Cr premaza za vezivanje. U odnosu na γ-TiAl supstrat prosečna mikrotvrdoća NiCr/YSZ premaza je povećana za faktor od oko 2. Test termalnog šoka pokazao je da kompozitna struktura ima superiornu snagu vezivanja, a da su defekti kao što su metalne kapljice na keramičkom premazu bile uzrok pukotina. Visoko energetski laser uništio je površinu γ-TiAl legure, formirajući izbačene produkte sagorevanja u zoni ablacije i raspršivanje ostatka oko zone ablacije. Kada je korišćen NiCr/YSZ premaz proces sagorevanja je bio odložen putem izolacije i rasipanja toplote. Opseg ablacije je bio kontrolisan i oštećenja od ablacije su smanjena pri istoj snazi zračenja. NiCr/YSZ premaz je prvobitno izrađen da bi poboljšao otpornost na toplotu γ-TiAl legure.

Ključne reči: *γ-TiAl legura; NiCr/YSZ premaz; Microstruktura; Snaga prijanjanja; Otpornost na toplotu*